

On the Effects of I/Q Imbalance on Sensing Performance in Full-Duplex Cognitive Radios

Alexandros–Apostolos A. Boulogeorgos*, Haythem A. Bany Salameh** and George K. Karagiannidis*[‡]

*Department of Electrical and Computer Engineering, Aristotle University of Thessaloniki, Greece, Emails: {ampoulog, geokarag}@auth.gr

**Telecommunications Engineering Department, Yarmouk University, Irbid 21163, Jordan, E-mail: haythem @ yu.edu.jo.

[‡]Department of Electrical and Computer Engineering, Khalifa University, Abu Dhabi, United Arab Emirates, Email: george.karagiannidis@kustar.ac.ae.

Abstract—Direct-conversion radio transceivers can offer re-programmable and low-cost hardware solutions for full-duplex (FD) cognitive radio (CR) devices. However, they are susceptible to radio frequency (RF) impairments, such as in-phase (I) and quadrature (Q) imbalance (IQI), which can significantly constrain the spectrum sensing capabilities. This paper is devoted to quantify and evaluate the effects of IQI in the context of spectrum sensing in FD CR systems, in which self-interference suppression (SIS) techniques are employed. Specifically, closed form expressions are derived for the false alarm and detection probabilities, under three different scenarios: imperfect SIS with joint transmitter (TX) and receiver (RX) IQI, imperfect SIS and ideal TX/RX RF front-end, and perfect SIS and ideal TX/RX RF front-end. The derived analytical results are validated through extensive simulations, which reveal that IQI has a detrimental impact on the spectrum sensing performance of the FD CR transceiver, which brings significant losses in the spectrum utilization.

I. INTRODUCTION

Cognitive radio (CR) systems have recently received considerable attention and have been adopted in wireless standards, such as long-term evolution (LTE) [1], [2]. In the traditional CR half-duplex (HD) mode, a CR device can either transmit or receive/sense, but not both, at a given time interval. However, full-duplex (FD) operation (i.e., transmit and receive/sense over the same frequency channel at the same time interval) by employing self-interference suppression (SIS) techniques, has been recently receive special attention (see for example [3], [4] and references therein).

One essential functionality in enabling efficient CR communications, whether operating in HD or FD mode, is spectrum sensing. The main objective of spectrum sensing is determining the temporarily vacant portions of spectrum. As a result, several studies were conducted to derive and analyze the spectrum sensing capabilities of optimal, sub-optimal, ad-hoc and cooperative solutions, assuming ideal radio frequency (RF) front-ends [5]–[10]. Yet, practical CR devices suffer from hardware imperfections, such as low-noise amplifier non-linearities, local oscillator phase noise and in phase (I) and quadrature (Q) imbalance (IQI) [11]–[17]. The aforementioned imperfections restrict the spectrum sensing capabilities of HD CR systems as demonstrated in [18]–[26]. More specifically, the authors in [18] investigated the effects of IQI on energy detection considering both cases of single- and multi-channel secondary user (SU) direct-conversion receiver (RX). It was shown that the false alarm probability in a

multi-channel environment significantly increases, compared to the ideal RF RX case. In [23], closed-form expressions for the detection and false alarm probabilities for Neyman-Pearson detector were derived for single-channel orthogonal frequency division multiplexing (OFDM) HD CR RX under joint transmitter (TX) and RX IQI. On the other hand, the effects of hardware imperfections in FD CR systems were studied in [27], where the problem was to find the achievable primary-cognitive rate region by studying the cognitive rate maximization problem. However, the impact of RF impairments on the spectrum sensing of the FD CR transceiver was not taken into consideration.

In this paper, we derive an analytical framework to evaluate the false-alarm and detection probabilities of energy detectors (ED) for a CR system operating in opportunistic spectrum access (OSA) FD mode, under SU's joint TX/RX IQI imperfections. Based on these metrics, we compare the spectrum sensing capabilities of the IQI FD CR with the ideal FD CR, under both cases of perfect and imperfect SIS, and the corresponding HD systems. Furthermore, to demonstrate the negative effects of IQI, the false alarm/detection probability are plotted for different IQI levels. Finally, simulations are provided to illustrate the accuracy of our analysis.

Notations: Unless otherwise stated, the operators $(\cdot)^*$, $\Re\{\cdot\}$ and $\Im\{\cdot\}$ represent the conjugation, real and imaginary parts of x , respectively. The operators $E[\cdot]$ and $|\cdot|$ denote the statistical expectation and the absolute value, respectively. Furthermore, $Q(x) = \frac{1}{\sqrt{2\pi}} \int_x^\infty e^{-t^2/2} dt$ stands for the Gaussian Q-function, whereas $Q^{-1}(x)$ denotes the inverse Q-function.

II. SYSTEM MODEL

As demonstrated in Fig. 1, we consider an OSA primary user (PU)/SU environment, where the CR devices operate in FD mode. Each SU device is considered to be a low-cost transceiver that suffers from joint TX/RX IQI. Furthermore, the SU i has partial SIS capability, measured by the degree of SIS $a_i \in [0, 1]$. Note that if $a_i = 0$, the SU has a complete SIS capability.

By denoting the two hypotheses, namely absent/present of PU, with the parameter $\theta \in \{0, 1\}$, the received baseband signal at the SU i can be expressed as

$$y_i(n) = \theta x_i(n) + a_i s_i(n) + w_i, \quad (1)$$

where $x_i(n)$, $s_i(n)$ and $w_i(n)$ are respectively the n -th sample of the I/Q imbalanced received PU signal by the i -th SU, the I/Q imbalanced received signal due to the SU's own transmission before applying SIS, and the I/Q imbalanced noise. These terms are given by [28]

$$x_i(n) = K_{1,i}^r x_{\text{id},i}(n) + K_{2,i}^r x_{\text{id},i}^*(n), \quad (2)$$

$$s_i(n) = \xi_{1,i} s_{\text{id},i}(n) + \xi_{2,i} s_{\text{id},i}^*(n) \quad (3)$$

and

$$w_i(n) = K_{1,i}^r w_{\text{id},i}(n) + K_{2,i}^r w_{\text{id},i}^*(n), \quad (4)$$

where $x_{\text{id},i}(n)$, $s_{\text{id},i}(n)$ and $w_{\text{id},i}(n)$ are respectively circularly symmetric complex white Gaussian (CSCWG) processes that model the received PU signal¹, the received signal due to the SU's own transmission before applying SIS and the received noise, respectively, under ideal RF front-end. The parameters $\xi_{1,i}$ and $\xi_{2,i}$ model the joint effect of TX/RX IQI and can be obtained by

$$\xi_{1,i} = K_{1,i}^r K_{1,i}^t + K_{2,i}^r (K_{2,i}^t)^*, \quad (5)$$

and

$$\xi_{2,i} = K_{1,i}^r K_{2,i}^t + (K_{1,i}^t)^* K_{2,i}^r. \quad (6)$$

Note that $K_{1,i}^t$, $K_{2,i}^t$, and $K_{1,i}^r$, $K_{2,i}^r$ stand for the TX and the RX IQI coefficients and are given by [28, Eqs. (5.23), (5.24), (5.29) and (5.30)]

$$K_{1,i}^t = \frac{1 + \epsilon_i^t e^{j\phi_i^t}}{2}, \quad K_{2,i}^t = \frac{1 - \epsilon_i^t e^{-j\phi_i^t}}{2}, \quad (7)$$

$$K_{1,i}^r = \frac{1 + \epsilon_i^r e^{-j\phi_i^r}}{2}, \quad K_{2,i}^r = \frac{1 - \epsilon_i^r e^{j\phi_i^r}}{2}, \quad (8)$$

with $\epsilon_i^{t/r}$ and $\phi_i^{t/r}$ denote the amplitude and phase imbalance at the TX/RX. Note that the IQI coefficients are connected as follows

$$K_{1,i}^{t/r} = 1 - (K_{2,i}^{t/r})^*. \quad (9)$$

The coefficients are also quantified using the image rejection ratio (IRR), which is defined as

$$\text{IRR}_i^{t/r} = \frac{|K_{1,i}^{t/r}|^2}{|K_{2,i}^{t/r}|^2}. \quad (10)$$

It is worth noting that for practical transceivers, the IRR is in the range of 20 – 40 dB [11]–[14], [16], [17]. Moreover, substituting (9) into (5) and (6), and after some algebraic manipulations, we obtain that

$$\xi_{1,i} = 1 - \xi_{2,i}^*. \quad (11)$$

Note that, for simplicity, we ignore the path loss between the SU's TX and its reception at the same node (i.e., $h_{ii} = 1$).

It is important to note that according to (1)–(4), the received signal at the i -th SU (y_i) is not only interfered by the transmitted signal $s_{\text{id},i}$, but it is also interfered by the signals $s_{\text{id},i}^*$ and $x_{\text{id},i}^*$, due to the effects of IQI.

¹This is a valid assumption that has also been employed in [18], [20], [25], [29], [30].

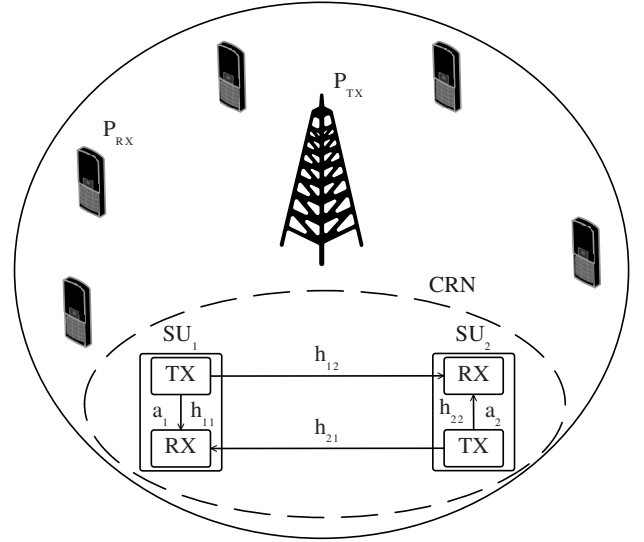


Fig. 1: System model for an SU link that opportunistically accesses the spectrum of a PU network.

III. FALSE ALARM AND DETECTION PROBABILITIES

We assume that the SU employs the classical ED, which calculates the test statistics according to

$$T_i = \frac{1}{N_s} \sum_{n=0}^{N_s-1} |y_i(n)|^2, \quad (12)$$

where N_s is the number of complex samples used for sensing. This test statistics are compared against a threshold (γ) to decide whether the channel is busy or idle, i.e., if $T_i < \gamma$ the ED decides that the channel is idle, otherwise it decides that it is busy.

Proposition 1. For a sufficient large number of samples, N_s , the conditional to θ distribution of the energy test statistics, when the SU has partial SIS and suffers from IQI can be well approximated by a Gaussian distribution with cumulative distribution function (CDF) obtained as

$$F(\gamma|\theta) = 1 - Q\left(\frac{\gamma - \mu_\theta}{\sqrt{\sigma_\theta^2}}\right), \quad (13)$$

where μ_θ and σ_θ^2 stand for the mean and variance of the test statistics, which are respectively given by

$$\begin{aligned} \mu_\theta &= \left(|K_{1,i}^r|^2 + |K_{2,i}^r|^2 \right) (\theta \sigma_{x_{\text{id}}}^2 + \sigma_{w_{\text{id}}}^2) \\ &+ a_i^2 \left(|\xi_{1,i}|^2 + |\xi_{2,i}|^2 \right) \sigma_{s_{\text{id}}}^2, \end{aligned} \quad (14)$$

and

$$\begin{aligned} \sigma_\theta^2 &= \frac{1}{N_s} \left(2\theta k_r \sigma_{x_{\text{id},i}}^4 + 2a_i^4 k_{t,r} \sigma_{s_{\text{id},i}}^4 + 2k_r \sigma_{w_{\text{id},i}}^4 \right. \\ &\left. + \theta k_{xw} \sigma_{x_{\text{id}}}^2 \sigma_{w_{\text{id}}}^2 + k_{xsw} (\theta \sigma_{x_{\text{id}}}^2 + \sigma_{w_{\text{id}}}^2) a_i^2 \sigma_{s_{\text{id}}}^2 - \mu_\theta^2 \right). \end{aligned} \quad (15)$$

Note that the coefficients k_r , k_{tr} and k_{xsw} are only related to the TX and RX IQI parameters, and can be expressed as

$$k_r = \left(|K_{1,i}^r|^4 + |K_{2,i}^r|^4 + 6 |K_{1,i}^r|^2 |K_{2,i}^r|^2 + 2\Re\{K_{1,i}^r\}^2 \Im\{K_{1,i}^r\}^2 + 2\Re\{K_{2,i}^r\}^2 \Im\{K_{2,i}^r\}^2 \right), \quad (16)$$

$$k_{tr} = \left(|\xi_{1,i}^r|^4 + |\xi_{2,i}^r|^4 + 6 |\xi_{1,i}^r|^2 |\xi_{2,i}^r|^2 + 2\Re\{\xi_{1,i}^r\}^2 \Im\{\xi_{1,i}^r\}^2 + 2\Re\{\xi_{2,i}^r\}^2 \Im\{\xi_{2,i}^r\}^2 \right), \quad (17)$$

$$k_{xsw} = \left((2\Re\{K_{1,i}^r\} - 1)^2 + 4\Im\{K_{1,i}^r\}^2 \right)^2 + 2 \left(|K_{1,i}^r|^2 + |K_{2,i}^r|^2 \right)^2 + 1, \quad (18)$$

and

$$k_{xsw} = \left((2\Re\{K_{1,i}^r\} - 1)^2 + 4\Im\{K_{1,i}^r\}^2 \right) \times \left((2\Re\{\xi_{1,i}^r\} - 1)^2 + 4\Im\{\xi_{1,i}^r\}^2 \right) + 2 \left(|K_{1,i}^r|^2 + |K_{2,i}^r|^2 \right) \left(|\xi_{1,i}^r|^2 + |\xi_{2,i}^r|^2 \right) + 1. \quad (19)$$

Proof: Since N_s is sufficiently large, the central limit theorem can be applied and, hence the distribution of the energy statistics can be approximated by a Gaussian distribution with mean and variance that are respectively given by

$$\mu_\theta = E[T_i | \theta] = \frac{1}{N_s} E \left[\sum_{n=0}^{N_s-1} |y_i(n)|^2 \right] = E[|y_i(n)|^2], \quad (20)$$

and

$$\sigma_\theta^2 = \text{Var}[T_i | \theta] = \frac{1}{N_s} \left(E[|y_i|^4] - \mu_\theta^2 \right). \quad (21)$$

By considering that x_i , s_i and w_i are uncorrelated random variable, (20) can be rewritten as

$$\mu_\theta = \theta E[|x_i|^2] + a_i^2 E[|s_i|^2] + E[|w_i|^2]. \quad (22)$$

Since $x_{id,i}$, $s_{id,i}$ and $w_{id,i}$ are zero mean CSCWG processes with uncorrelated real and imaginary parts and variances $\sigma_{x_{id,i}}^2 = E[|x_{id,i}|^2]$, $\sigma_{s_{id,i}}^2 = E[|s_{id,i}|^2]$ and $\sigma_{w_{id,i}}^2 = E[|w_{id,i}|^2]$, x_i , s_i and w_i are random uncorellated processes with variances given by

$$E[|x_i|^2] = \left(|K_{1,i}^r|^2 + |K_{2,i}^r|^2 \right) \sigma_{x_{id,i}}^2, \quad (23)$$

$$E[|s_i|^2] = \left(|\xi_{1,i}^r|^2 + |\xi_{2,i}^r|^2 \right) \sigma_{s_{id,i}}^2, \quad (24)$$

and

$$E[|w_i|^2] = \left(|K_{1,i}^r|^2 + |K_{2,i}^r|^2 \right) \sigma_{w_{id,i}}^2. \quad (25)$$

Substituting (23)–(25) into (22) and after some mathematical manipulations, we obtain the result in (14).

Nevertheless, to derive the variance of the test statistics, we need to evaluate $E[|y_i|^4]$, which can be obtained using (1) as follows

$$E[|y_i|^4] = \theta E[|x_i|^4] + a_i^4 E[|s_i|^4] + E[|w_i|^4] + 2a_i^2 \theta E[|x_i|^2] E[|s_i|^2] + 2\theta E[|x_i|^2] E[|w_i|^2] + 2a_i^2 E[|s_i|^2] E[|w_i|^2] + 4E \left[\left(\Re\{\theta a_i x_i s_i^* + \theta x_i w_i^* + a_i s_i w_i^*\} \right)^2 \right], \quad (26)$$

where, according to (2)–(4), and after some algebraic manipulations, $E[|x_i|^4]$, $E[|s_i|^4]$ and $E[|w_i|^4]$ can be expressed as

$$E[|x_i|^4] = 2k_r \sigma_{x_{id,i}}^4, \quad (27)$$

$$E[|s_i|^4] = 2k_{t,r} \sigma_{s_{id,i}}^4, \quad (28)$$

and

$$E[|w_i|^4] = 2k_r \sigma_{w_{id,i}}^4. \quad (29)$$

Moreover,

$$E \left[\left(\Re\{\theta a_i x_i s_i^* + \theta x_i w_i^* + a_i s_i w_i^*\} \right)^2 \right] = \theta a_i^2 E[\Re\{x_i\}^2] E[\Re\{s_i\}^2] + a_i^2 \theta E[\Im\{x_i\}^2] E[\Im\{s_i\}^2] + \theta E[\Re\{x_i\}^2] E[\Re\{w_i\}^2] + \theta E[\Im\{x_i\}^2] E[\Im\{w_i\}^2] + a_i^2 E[\Re\{s_i\}^2] E[\Re\{w_i\}^2] + a_i^2 E[\Im\{s_i\}^2] E[\Im\{w_i\}^2]. \quad (30)$$

Next, we derive $E[\Re\{x_i\}^2]$, $E[\Re\{s_i\}^2]$, $E[\Re\{w_i\}^2]$, $E[\Im\{x_i\}^2]$, $E[\Im\{s_i\}^2]$ and $E[\Im\{w_i\}^2]$. By using (9), (11) and the fact that

$$E[\Re\{x_{id,i}\}^2] = E[\Im\{x_{id,i}\}^2] = \frac{\sigma_{x_{id,i}}^2}{2}, \quad (31)$$

$$E[\Re\{s_{id,i}\}^2] = E[\Im\{s_{id,i}\}^2] = \frac{\sigma_{s_{id,i}}^2}{2} \quad (32)$$

and

$$E[\Re\{w_{id,i}\}^2] = E[\Im\{w_{id,i}\}^2] = \frac{\sigma_{w_{id,i}}^2}{2}, \quad (33)$$

we show that

$$E[\Re\{x_i\}^2] = \frac{\sigma_{x_{id,i}}^2}{2}, \quad (34)$$

$$E[\Re\{s_i\}^2] = \frac{\sigma_{s_{id,i}}^2}{2}, \quad (35)$$

$$E[\Re\{w_i\}^2] = \frac{\sigma_{w_{id,i}}^2}{2}. \quad (36)$$

$$E[\Im\{x_i\}^2] = \left((2\Re\{K_{1,i}^r\} - 1)^2 + 4\Im\{K_{1,i}^r\}^2 \right) \frac{\sigma_{x_{id,i}}^2}{2}, \quad (37)$$

$$E[\Im\{s_i\}^2] = \left((2\Re\{\xi_{1,i}^r\} - 1)^2 + 4\Im\{\xi_{1,i}^r\}^2 \right) \frac{\sigma_{s_{id,i}}^2}{2}, \quad (38)$$

and

$$E [\Im\{w_i\}^2] = \left((2\Re\{K_{1,i}^r\} - 1)^2 + 4\Im\{K_{1,i}^r\}^2 \right) \frac{\sigma_{w_{id}}^2}{2}. \quad (39)$$

Substituting (34)–(39) into (30) and then to (26) and (21), we get (15). This concludes the proof. ■

Note that the exact distribution of T_i is rather complicated because of the dependency between the random variable, namely $\Re\{y_i\}$ and $\Im\{y_i\}$, due to the effects of IQI.

Using the derived distribution for the test statistics, the false alarm and the detection probability, when the SU has partial SIS and suffers from IQI, can be derived by

$$P_{fa} = P_r(T > \gamma | \theta = 0) = Q \left(\frac{\gamma - \mu_0}{\sqrt{\sigma_0^2}} \right), \quad (40)$$

and

$$P_d = P_r(T > \gamma | \theta = 1) = Q \left(\frac{\gamma - \mu_1}{\sqrt{\sigma_1^2}} \right). \quad (41)$$

For a target false alarm probability \tilde{P}_{fa} , the energy threshold can be evaluated using (40) as follows

$$\tilde{\gamma} = \sqrt{\sigma_0^2} Q^{-1}(\tilde{P}_{fa}) + \mu_0. \quad (42)$$

In this case, the detection probability, based on (41) is given by

$$\tilde{P}_d = Q \left(\frac{\sqrt{\sigma_0^2} Q^{-1}(\tilde{P}_{fa}) + \mu_0 - \mu_1}{\sqrt{\sigma_1^2}} \right). \quad (43)$$

Remark 1. In case of imperfect SIS and ideal TX/RX RF front end, the mean and variance of the SU received signal are given by

$$\mu_\theta^2 = \theta\sigma_{x_{id}}^2 + a_i^2\sigma_{s,id}^2 + \sigma_{w_{id}}^2, \quad (44)$$

and

$$\sigma_\theta^2 = \frac{\mu_\theta^2}{N_s}. \quad (45)$$

Proof: In case of ideal TX/RX RF front-ends $K_{1,i}^t = K_{1,i}^r = 1$ and $K_{2,i}^t = K_{2,i}^r = 0$. Consequently, $\xi_{1,i} = 1$ and $\xi_{2,i} = 0$. Hence, based on (16)–(19), $k_r = k_{tr} = 1$ and $k_{xw} = k_{xsw} = 4$. Substituting these values in (14) and (15), and after some algebraic manipulations, we get (44) and (45), respectively. This concludes the proof. ■

Remark 2. In case of perfect SIS and ideal TX/RX SU RF front-ends, the mean and variance of the SU received signal are given by

$$\mu_\theta^2 = \theta\sigma_{x_{id}}^2 + \sigma_{w_{id}}^2, \quad (46)$$

and

$$\sigma_\theta^2 = \frac{\mu_\theta^2}{N_s}. \quad (47)$$

Proof: In case of ideal RF front-end and perfect SIS, $K_{1,i}^t = K_{1,i}^r = \xi_{1,i} = 1$, $K_{2,i}^t = K_{2,i}^r = \xi_{2,i} = 0$ and $a_i = 0$.

By substituting these values in (14) and (15), we get (46) and (47), respectively. This concludes the proof. ■

Note that (46) coincide with [18, Eq.3], which refer to an ideal RF front-end HD CR system. In other words, in case of ideal RF front-end transceivers, regardless of whether the system operates in HD or FD mode with perfect SIS, the EDs provides the same spectrum sensing performance.

Remark 3. In case of perfect SIS and TX/RX I/Q imbalanced RF front-ends, the mean and variance of the SU received signal are respectively given by

$$\mu_\theta^2 = \left(|K_{1,i}^r|^2 + |K_{2,i}^r|^2 \right) (\theta\sigma_{x_{id}}^2 + \sigma_{w_{id}}^2), \quad (48)$$

and

$$\sigma_\theta^2 = \frac{2\theta k_r \sigma_{x_{id},i}^4 + 2k_r \sigma_{w_{id},i}^4 + \theta k_{xw} \sigma_{x_{id}}^2 \sigma_{w_{id}}^2 - \mu_\theta^2}{N_s}. \quad (49)$$

Proof: In case of non-ideal RF front-ends and perfect SIS, $a_i = 0$. Substituting $a_i = 0$ into (14) and (15), we get (48) and (49), respectively. This concludes the proof. ■

IV. NUMERICAL EVALUATION AND DISCUSSION

In this section, we demonstrate the effects of IQI on the spectrum sensing performance of EDs by illustrating analytical and computer simulation results for different IQI and SIS levels. In particular, we consider the following insightful scenario. We consider that the SNR of the received ideal signal at the SU i , $i \in \{1, 2\}$, due to the PU activity is -15 dB, while before applying a SIS technique, the self-interference to noise ratio (INR) due to the transmission of the SU i is set to 20 dB and the degree of SIS is set to 0.01 (i.e., 40 dB). Furthermore, to decide whether the channel is busy or idle, the ED is assumed to use $N_s = 8 \times 10^3$ samples. It should be noted that all the plotted figures contain both the analytical and simulation results, which are represented by solid lines and discrete marks, respectively.

In Fig. 2, the false alarm probability is plotted versus the energy detection threshold for different values of IRR considering that both TX and RX suffer from the same levels of IQI. This figure shows that the analytical results perfectly match the simulation results. This verifies the presented analytical framework. Moreover, it is observed that as IRR decreases, the energy threshold to achieve a target false alarm probability increases. For instance, if the target false alarm probability threshold is 0.1 , then in case of ideal RF front-end, the energy threshold should be set to 0.85 dB. In case of a non-ideal CR device with $IRR = 25$ dB, it should be shifted about 0.2 dB and should be set to 1.05 dB. This may not seem to be a significant shift, yet, if the effects of IQI is not taken into consideration the false alarm probability of the system reaches 1 . This observation reveals and demonstrates the importance of the derived expressions.

Fig. 3 illustrates the impact of IQI in the detection performances of the FD CR device. Specifically, the detection probability is plotted against the energy threshold for different levels of IQI, considering that both the TX and RX have the

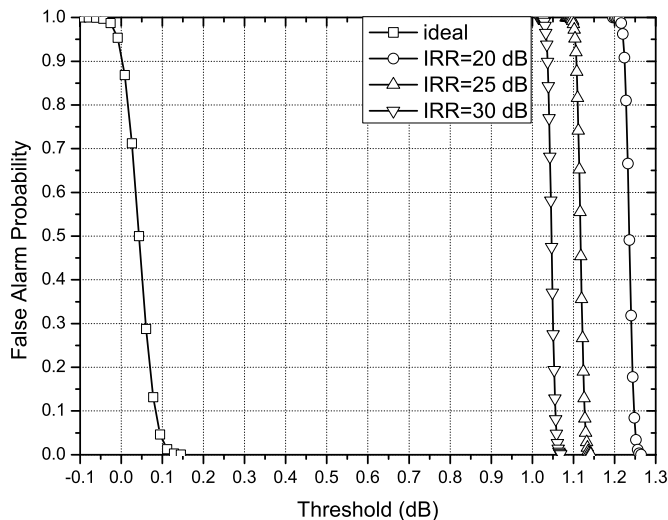


Fig. 2: The false alarm probability as a function of the energy threshold for different values of IRR and $a_1 = a_2 = 0.01$.

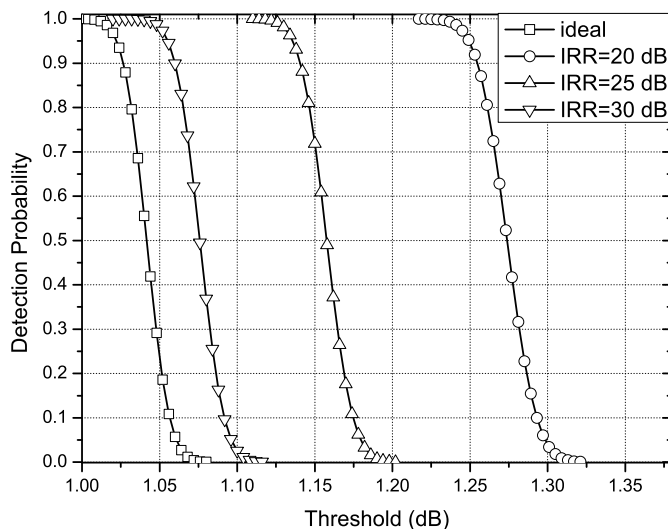


Fig. 3: The detection probability as a function of the energy threshold for different values of IRR and $a_1 = a_2 = 0.01$.

same IRR. We observe that as IRR decreases, the interference due to IQI increases. Hence, for a given energy threshold, the detection probability increases. For example, for $\gamma = 1.05$ dB, in case of ideal RF front-end the detection probability is about 0.2. On the other hand, in case of I/Q imbalanced RF front-end with IRR = 25 dB and for the same energy threshold, the detection probability equals to 1. In addition, if the target false alarm probability is set to 0.1, then in case of ideal RF front-end the detection probability equals to 1. For the same target and in case of non-ideal RF front-end with IRR = 20 dB, the energy threshold should be set to 1.257 dB, which results in a the detection probability of 0.87. This example indicates that the spectrum sensing capabilities of the FD CR ED are constrained due to IQI.

V. CONCLUSIONS

This paper investigated the spectrum sensing performance of OSA FD CR system, when the SUs' devices employing SIS techniques and suffer from joint TX/RX IQI. We have derived closed-form expressions for the false alarm and the detection probabilities under realistic scenarios of non-perfect SIS and transceivers' RF front-end impairments. Our results illustrated the significant degrading effects of IQI on the ED spectrum sensing performance, which results in significant losses in spectrum utilization. Therefore, IQI should be carefully taken into consideration when designing FD CR devices.

REFERENCES

- [1] J. Xiao, R. Hu, Y. Qian, L. Gong, and B. Wang, "Expanding LTE network spectrum with cognitive radios: From concept to implementation," *IEEE Wireless Commun. Mag.*, vol. 20, no. 2, pp. 12–19, Apr. 2013.
- [2] H. Bany Salameh, "Efficient resource allocation for multi-cell heterogeneous cognitive networks with varying spectrum availability," *IEEE Transactions on Vehicular Technology*, 2015.
- [3] W. Afifi and M. Krunz, "Incorporating self-interference suppression for full-duplex operation in opportunistic spectrum access systems," *IEEE Trans. Wireless Commun.*, vol. 14, no. 4, pp. 2180–2191, Apr. 2015.
- [4] E. Askari and S. Aissa, "Full-duplex cognitive radio with packet fragmentation," in *IEEE Wireless Communications and Networking Conference (WCNC)*, Apr. 2014, pp. 1502–1507.
- [5] T. Yucek and H. Arslan, "A survey of spectrum sensing algorithms for cognitive radio applications," *IEEE Communications Surveys Tutorials*, vol. 11, no. 1, pp. 116–130, Jan. 2009.
- [6] O. Altrad, S. Muhaidat, A. Al-Dweik, A. Shami, and P. Yoo, "Opportunistic spectrum access in cognitive radio networks under imperfect spectrum sensing," *IEEE Trans. Veh. Technol.*, vol. 63, no. 2, pp. 920–925, Feb. 2014.
- [7] L. Fan, X. Lei, T. Duong, R. Hu, and M. ElKashlan, "Multiuser cognitive relay networks: Joint impact of direct and relay communications," *IEEE Trans. Wireless Commun.*, vol. 13, no. 9, pp. 5043–5055, Sep. 2014.
- [8] S. Huang, X. Liu, and Z. Ding, "Optimal sensing-transmission structure for dynamic spectrum access," in *IEEE INFOCOM*, April 2009, pp. 2295–2303.
- [9] S. Atapattu, C. Tellambura, and H. Jiang, "Energy detection based cooperative spectrum sensing in cognitive radio networks," *IEEE Trans. Wireless Commun.*, vol. 10, no. 4, pp. 1232–1241, April 2011.
- [10] M. Shakir, A. Rao, and M.-S. Alouini, "Generalized mean detector for collaborative spectrum sensing," *IEEE Trans. Commun.*, vol. 61, no. 4, pp. 1242–1253, Apr. 2013.
- [11] B. Razavi, *RF microelectronics*. Prentice Hall New Jersey, 1998, vol. 1.
- [12] S. Mirabbasi and K. Martin, "Classical and modern receiver architectures," *IEEE Commun. Mag.*, vol. 38, no. 11, pp. 132–139, Nov 2000.
- [13] L. Anttila, M. Valkama, and M. Renfors, "Circularity-based I/Q imbalance compensation in wideband direct-conversion receivers," *IEEE Trans. Veh. Commun.*, vol. 57, no. 4, pp. 2099–2113, July 2008.
- [14] A.-A. A. Boulogeorgos, P. C. Sofotasios, S. Muhaidat, M. Valkama, and G. K. Karagiannidis, "The effects of RF impairments in Vehicle-to-Vehicle communications," in *IEEE 25th International Symposium on Personal, Indoor and Mobile Radio Communications - (PIMRC): Fundamentals and PHY (IEEE PIMRC 2015 - Fundamentals and PHY)*, Hong Kong, P.R. China, Aug. 2015.
- [15] M. Mokhtar, A.-A. A. Boulogeorgos, G. K. Karagiannidis, and N. Al-Dhahir, "OFDM Opportunistic Relaying Under Joint Transmit/Receive I/Q Imbalance," *IEEE Trans. Commun.*, vol. 62, no. 5, pp. 1458–1468, May 2014.
- [16] A. A. Boulogeorgos, V. M. Kapinas, G. K. Karagiannidis, and R. Schober, "I/Q-imbalance self-interference coordination," *CoRR*, vol. abs/1507.05352, 2015. [Online]. Available: <http://arxiv.org/abs/1507.05352>
- [17] A.-A. A. Boulogeorgos, P. C. Sofotasios, B. Selim, S. Muhaidat, G. K. Karagiannidis, and M. Valkama, "Effects of RF impairments in communications over cascaded fading channels," *IEEE Trans. Veh. Technol.*, vol. PP, no. 99, 2016.

- [18] A. Gokceoglu, S. Dikmese, M. Valkama, and M. Renfors, "Energy detection under IQ imbalance with single- and multi-channel direct-conversion receiver: Analysis and mitigation," *IEEE J. Sel. Areas Commun.*, vol. 32, no. 3, pp. 411–424, Mar. 2014.
- [19] B. Razavi, "Cognitive radio design challenges and techniques," *IEEE J. Solid-State Circuits*, vol. 45, no. 8, pp. 1542–1553, Aug. 2010.
- [20] A. Gokceoglu, Y. Zou, M. Valkama, and P. Sofotasios, "Multi-channel energy detection under phase noise: analysis and mitigation," *Mobile Networks and Applications*, vol. 19, no. 4, pp. 473–486, Aug. 2014.
- [21] J. Verlant-Chenet, J. Renard, J.-M. Dricot, P. De Doncker, and F. Horlin, "Sensitivity of spectrum sensing techniques to rf impairments," in *IEEE 71st Vehicular Technology Conference (VTC 2010-Spring)*, May 2010, pp. 1–5.
- [22] A. Zahedi-Ghasabeh, A. Tarighat, and B. Daneshrad, "Cyclo-stationary sensing of ofdm waveforms in the presence of receiver rf impairments," in *IEEE Wireless Communications and Networking Conference (WCNC)*, Apr. 2010, pp. 1–6.
- [23] A. ElSamadouny, A. Gomaa, and N. Al-Dhahir, "Likelihood-based spectrum sensing of OFDM signals in the presence of Tx/Rx I/Q imbalance," in *IEEE Global Communications Conference (GLOBECOM)*, Dec. 2012, pp. 3616–3621.
- [24] O. Semiari, B. Maham, and C. Yuen, "Effect of I/Q imbalance on blind spectrum sensing for OFDMA overlay cognitive radio," in *1st IEEE International Conference on Communications in China (ICCC)*, Aug 2012, pp. 433–437.
- [25] A.-A. A. Boulogeorgos, N. Chatzidiamantis, G. K. Karagiannidis, and L. Georgiadis, "Energy detection under RF impairments for cognitive radio," in *IEEE ICC 2015 - Workshop on Cooperative and Cognitive Networks (CoCoNet) (ICC'15 - Workshops 16)*, London, United Kingdom, Jun. 2015, pp. 955–960.
- [26] A.-A. A. Boulogeorgos, N. D. Chatzidiamantis, and G. K. Karagiannidis, "Spectrum sensing under hardware constraints," *CoRR*, vol. abs/1510.06527, 2015. [Online]. Available: <http://arxiv.org/abs/1510.06527>
- [27] G. Zheng, I. Krikidis, and B. Ottersten, "Full-duplex cooperative cognitive radio with transmit imperfections," *IEEE Transactions on Wireless Communications*, vol. 12, no. 5, pp. 2498–2511, May 2013.
- [28] T. Schenk, *RF Imperfections in High-Rate Wireless Systems*. The Netherlands: Springer, 2008.
- [29] S. Chatterjee, S. Maity, and T. Acharya, "Energy efficient cognitive radio system for joint spectrum sensing and data transmission," *IEEE Journal on Emerging and Selected Topics in Circuits and Systems*, vol. 4, no. 3, pp. 292–300, Sep. 2014.
- [30] N. Mahmood, F. Yilmaz, G. Oien, and M.-S. Alouini, "On hybrid cooperation in underlay cognitive radio networks," *IEEE Trans. Wireless Commun.*, vol. 12, no. 9, pp. 4422–4433, Sep. 2013.